Material and doping dependence of the nodal and anti-nodal dispersion renormalizations in single- and multi-layer cuprates

S. Johnston[1,3], W. S. Lee[2,3], Y. Chen[3,4], E. A. Nowadnick[3,5], B. Moritz[3,6], Z.-X. Shen[2,3,5,7], and T. P. Devereaux[2,3]
[1]*Department of Physics and Astronomy, University of Waterloo, Waterloo, ON N2L 3G1, Canada*
[2]*Geballe Laboratory for Advanced Materials, Stanford University, Stanford, CA 94305, USA*
[3]*Stanford Institute for Materials and Energy Science, SLAC National Accelerator Laboratory and Stanford University, Stanford, CA 94305, USA*
[4]*Advanced Light Source, Lawrence Berkeley National Laboratory, Berkeley, CA 94720, USA*
[5]*Department of Physics, Stanford University, Stanford, CA 94305, USA*
[6]*Department of Physics and Astrophysics, University of North Dakota, Grand Forks, ND 58202, USA and*
[7]*Department of Applied Physics, Stanford University, Stanford, CA 94305, USA*
(Dated: December 15, 2009)

In this paper we present a review of bosonic renormalization effects on electronic carriers observed from angle-resolved photoemission spectra in the cuprates. Specifically, we discuss the viewpoint that these renormalizations represent coupling of the electrons to the lattice and review how materials dependence, such as the number of CuO_2 layers, and doping dependence can be understood straightforwardly in terms of several aspects of electron-phonon coupling in layered correlated materials.

I. INTRODUCTION

The discovery of a "kink" in the nodal ((0,0) - (π,π)) dispersion of the high-T_c cuprates, and band renormalizations, in the form of a peak-dip-hump structure in the anti-nodal (0,π) - (π,π) dispersion,[1–18] have attracted considerable attention in recent years. These band renormalizations have been interpreted as due to electron-boson coupling, and it is believed that understanding origin of these renormalizations will provide crucial information about the underlying pairing mechanism in these materials. There is still considerable debate as to number and to the identity of the responsible bosonic mode(s) and whether these modes might be relevant to superconductivity[19].

In terms of coupling to a bosonic mode, the candidate modes have been associated with either coupling to electron spins or to the lattice. Both viewpoints have their merits and at present the debate is unsettled. Initially the kinks had been associated with coupling to a collective mode found in neutron scattering near antiferromagnetic (AF) momentum transfers (π,π), the so called magnetic resonance mode.[4,9,11,12] The basis for the association was mainly due to the observation that the mode, as well as the kinks, were largely found only below the superconducting transition temperature. However, since then it has been realized that the kink features exist both above and below T_c. Furthermore, the relatively narrow momentum range of the mode itself implies that the renormalizations should be relatively localized to impact electrons in a narrow region of the Fermi surface (FS) near the AF zone boundary. Given that kinks have been observed throughout the Brillouin zone (BZ), some of the original advocates of coupling to the neutron resonance mode indicate that this mode cannot be the mode responsible for the observed kink in the nodal direction.[20]

The renormalizations could also be due to coupling of electrons a damped magnon continuum, which have less well-defined momentum structure. This has the appeal that as the magnons become better defined nearing the AF phase, the strength of the kinks would be expected to increase, in agreement with experiments. However, the strength of the coupling of magnons to electrons is still under debate.[21,22] For example, quantitative comparisons of angle-resolved photoemission spectroscopy (ARPES) and neutron measurements on $YBa_2Cu_3O_{6.6}$ (YBCO) have been made, and the overall strength of the coupling inferred from the data was indicated to be of sufficient strength to give rise to superconductivity.[17] We remark that a quantitative comparison between the neutron scattering and ARPES measurements reported in Ref. 17 can be complicated by the polar surface of cleaved YBCO (as opposed to Bi- and Tl-compounds which have no polar surface) resulting in a surface reconstruction with the potential to produce significant differences between the bulk and surface layers of this material. This leads to an inconsistency where the FS revealed from ARPES matches that of an overdoped material, while the neutron scattering spectra used in the phenomenology was obtained on an underdoped material exhibiting a pseudogap. Since this comparison has only been performed on one cuprate, which has the abovementioned issues, we believe that at present the issue remains open.

A non-bosonic origin of the kink has been proposed whereby the kink is produced by many-body correlations.[23] The energy scale of the renormalization is set by the strength of the quasiparticle residue Z and is generic to any strongly correlated material with a sizable Hubbard interaction. Since the correlation strength is set by the a combination of the charge transfer energy to move a hole from copper to oxygen in the cuprates, the kink strength and position would be then fairly universal across the cuprate family.

A systematic examination of the effects of doping, material class, and temperature have not been thoroughly explored. In fact, given that both the electronic correla-

Work supported in part by US Department of Energy contract DE-AC02-76SF00515.

tions and the spin continuum arises from the CuO_2 plane, one might expect the coupling to electrons which might give rise to a putative kink to be relatively material-class independent. On the other hand, it is well-known that a neutron resonance displays a material dependence, appearing at larger energies for larger T_c materials including both the single and multi-layer cuprates. This opens the possibility of linking the neutron resonance with ARPES renormalizations via a material-dependent study.

An alternative proposal is coupling to a spectrum of oxygen vibrational phonon modes,[3,7,25,26] specifically, the c-axis out-of-phase bond-buckling oxygen vibration or B_{1g} mode ($\Omega \sim 35 - 45$ meV) and the in-plane bond-stretching oxygen mode ($\Omega \sim 70 - 80$ meV). This multi-phonon proposal has been able to account for many experimental observations including the anisotropy of the observed renormalizations,[25] fine structure in the form of subkinks observed in the temperature dependence of the self-energy in $Bi_2Sr_2CaCu_2O_{8+\delta}$ (Bi-2212)[26], which track the opening of the superconducting gap, and doping dependent changes in the self-energy.[15,29] This interpretation is further supported by recent ARPES experiments that have measured an $^{16}O \rightarrow {}^{18}O$ isotope shift in the nodal kink position.[24]

In general, the energy scale of the kink for a d-wave superconductor coupled to an Einstein mode occurs at $\Omega + \Delta_0$ where Ω is the energy of the mode and Δ_0 is the maximum value of the superconducting gap. This is independent of the identity of the mode, such as phonons or for a spin resonance mode for example, and arises from the large density of states pile-up at the gap edge Δ_0 below T_c.[25–28] An exception arises in the limit of extreme forward scattering by the mode, where the coupling constant becomes sharply peaked at $\mathbf{q} = 0$.[30] Theoretical work has shown that correlations can enhance the electron-phonon coupling vertex for small momentum transfer leading to a coupling which favors forward scattering.[31,32] In the nodal region, where the gap is zero, such a coupling will produce a peak in the self-energy at the mode energy Ω. However, such a peak would gap shift as a function of momentum following the momentum dependence of the gap away from the node. Since the energy scale of the kink does not exhibit a dispersion in the vicinity of the node one can conclude that the enhancement of the $\mathbf{q} = 0$ el-ph vertex is not sharp enough to produce the strong forward scattering assumed in Ref. 30.

The phonon scenario has been criticized using evidence based on density functional theory (DFT) approaches, which have traditionally not provided evidence of strong electron-phonon coupling in YBCO and $La_{2-x}Sr_xCuO_4$ (see Refs. 33–35 for recent works). LDA predicts the total coupling to all the modes to be less than one, and when a self energy calculated within the Migdal limit is compared to nodal ARPES cuts in the cuprates, it was found that the coupling was too small by a factor of 3-5 to account for the observed kinks. However, while DFT has done a remarkably good job of predicting phonon dispersions, the width of the phonon lineshapes are underestimated in most cases in comparison with experiment, sometimes by an order of magnitude.[36] This is not unexpected given that DFT predicts metallic behavior for un-doped cuprates and does not account for the factor of five reduced bandwidth over DFT values observed in optimally doped Bi-2212.[37] A simple reduction of the bandwidth might account for the discrepancy. It is not clear if these findings indicate that lattice effects are small or that DFT-based approaches alone are inadequate to the represent the physics of the cuprates.

Analogous features to those observed in ARPES have been observed in scanning tunneling microscopy (STM). These features have also been interpreted in terms of coupling to a bosonic mode,[38–41] and possibly the same mode responsible for the ARPES observed kink. As with the kink observed in the single-particle dispersion by ARPES, the origin of this feature remains a source of debate.[42,43] Pilgram *et al.*[42] invoke a co-tunneling mechanism between the tip and sample via an apical oxygen pathway. Taking this view, the modulations in the STM derived density of states (DOS) are unrelated to the physics of the CuO_2 plane. In contrast, the observed STM spectra look similar in Bi-2212 (which has an apical oxygen) and $Ca_{2-x}Na_xCuO_2Cl_2$[44] (which doesn't) indicating that the tunneling pathway from the STM tip to the conduction electrons does seem to be that critical, and that the renormalizations observed in both STM and ARPES could have a common origin. Ref. 38 also reported an ^{18}O isotope shift of the feature in a Bi-2212 sample. While at face value this would indicate a lattice origin to the renormalizations in the tunneling spectra, this too remains controversial.[20] Therefore, even though there exists a wide array of experimental data from ARPES and other probes, it is clear that the identity of the bosonic mode is still hotly debated.

It would take much too much space to review each and every interpretation of each and every experimental observation relating to kinks, and it is not clear if such a review would be useful. Rather than attempting to outline all possible scenarios, we instead present a review of ways in which different scenarios may be differentiated by studying the material, doping and temperature dependence of the band renormalizations. We admit at the outset our bias - that the electronic renormalizations are best interpreted in terms of coupling to the lattice. As there are many articles advocating other points of view, and this volume is organized according to the effects of electron-phonon coupling in the cuprates, our choice of presentation is thusly defined.

This work will focus is on how c-axis phonons provide a material dependence to the ARPES kinks due to the phonon's sensitivity to local symmetry and the environment surrounding the CuO_2 plane. We consider doping dependent changes to the renormalization in Bi-2212 as well as the dependence of these renormalizations within the Bi and Tl families as the number of CuO_2 layers is

varied. We will also discuss some recent ARPES results on the $n = 4$ layer system $Ba_2Ca_3Cu_4O_8F_2$ (F0234).[45] In this system, the inner and outer layers occupy different crystal environments resulting in differing Madelung energies associated with each plane in the undoped compound. This difference drives inequivalent dopings between the two sets of layers, with one set n-type and the other p-type. The inequivalent doping in each plane generates further symmetry breaking in the layers and the el-ph coupling in each layer is expected to differ. Indeed, Ref. 45 observes stronger kink features in the plane associated with the outer (n-type) layer of the material. Here, we will discuss these observations in the context of the el-ph coupling scenario.

The organization of this paper is follows. In section II we discuss the role of symmetry breaking in producing el-ph coupling to c-axis phonons and how such coupling is expected to vary with the crystal structure of the high-T_c cuprates. In section III we present ARPES data for various multi-layer cuprates in order to examine how band renormalizations vary with the number of CuO_2 layers. Of particular interest are the results for the single layer Tl cuprate Tl-2201. Here, we show that Tl-2201 does not resolve the typical peak-dip-hump structures in the antinodal region despite the fact that the spin resonance mode exists in this system.[46] In section IV the doping dependence of the nodal and antinodal dispersions for Bi-2122 are presented. The renormalizations in each region behave differently as the samples are overdoped, pointing to presence of multiple bosonic modes. In section V we present aspects of the nodal kink for the multi-layer F-family of cuprates. Electronic dispersions for the p-bands of the F-family are presented together with a theoretical basis for understanding the self-doping phenomena in $Ba_2Ca_3Cu_4O_8F_2$ (F0234). We also discuss what implications this process has on coupling to c-axis phonons. Finally, in section VI, we conclude with a brief summary and some additional remarks.

II. ELECTRON-PHONON COUPLING IN MULTI-LAYER CUPRATES

In this section we discuss how c-axis phonons can be sensitive to the material environment off the CuO_2 planes. There are many different sorts of phonons in the layered cuprates, however not all of these modes are expected to be sensitive to carrier concentration (such as those involving atoms in the charge reservoirs), and of those involving Cu and O, only a subset may be expected to vary across cuprate materials and family classes. Deformation electron-phonon (el-ph) coupling, involving in-plane bond-stretching modes for example,[47] depends on the Cu-O bond distance which is relatively constant in all cuprates. Therefore coupling to these modes is expected to be relatively material independent. They can be doping dependent however due to either correlation effects or to the changeover from 2D to 3D transport with increased hole concentration which changes the character of charge screening. However, a clear material dependence may arise for modes which electrostatically couple to the Madelung environment coming from all ions in the unit cell. This sort of coupling is believed to be most relevant for c-axis bond buckling modes such as the out-of-phase planar oxygen vibration (which is $B_{1g,1u}$ Raman,infrared active in multi-layer cuprates), or the in-phase ($A_{1g,1u}$ vibration of the planar oxygen atoms. These modes have been studied extensively in the context Raman, infrared and neutron spectroscopy[48–50] Although the nomenclature only holds for Raman $\mathbf{q} = 0$ momentum transfers, we denote the out-of-phase mode as the "B_{1g}" mode, and the in-phase mode "A_{1g}".[48] Since our goal is to explore the materials dependence of the band renormalizations, we will focus our attention to the c-axis modes.

El-ph coupling to c-axis phonons can arise due to the modulated Madelung environment the ion feels. If the ion sits in a mirror plane, such as the oxygens in the CuO_2 plane in an ideal single layer cuprate, the Madelung energy is at a local minima and the modulation of the energy and the coupling must be of second order in the ion displacements.[25,48,51] However, steric forces may force the CuO_2 to buckling along the c-axis which then creates a coupling to linear order in the displacements.[53] In terms of material dependence, such steric forces are present in all CuO_2 systems and therefore do not contribute to differences between materials. Another second pathway for mirror symmetry breaking can occur locally by introducing substitutional or interstitial dopant atoms in the charge reservoir area off the CuO_2 planes. These dopants donate charge to the CuO_2 plane(s), and cast c-axis electric fields E_z that are poorly screened by the in-plane carriers.[52] Through this mechanism, coupling to c-axis phonons can occur in single layer systems where they are normally forbidden by symmetry. This would then lead to a doping-dependence electron-phonon coupling.

This is to be contrasted with multi-layer cuprates, where even in an ideal material the CuO_2 plane does not necessarily lie in a mirror plane (for odd number of CuO_2 layers there will always been one CuO_2 plane which lies in the mirror plane) and a coupling which is first order in the c-axis displacement is expected, whereby the strength of the coupling is determined by the spatial variation of the Madelung energy along the c-axis. This is characterized by the local crystal field E_z which varies from material to material with the chemical environment (number of layers and doping from the ideal stoichiometric compound). The strength of the coupling to these modes scales as $\lambda \propto E_z^2$. Due to the oxygen charge transfer form factors, it has been shown that the B_{1g} mode couples most strongly to antinodal electrons[25]. This is the case for the spin resonance mode due to its strong tendency to scatter electrons near the AF zone boundary. Therefore, the material dependence of the anti-nodal electrons offers a straightforward way to distinguish between these two scenarios.

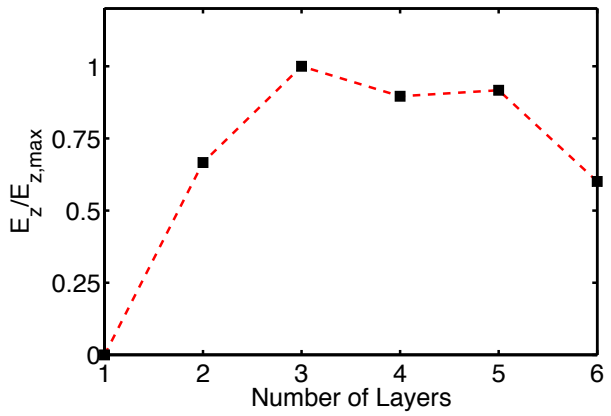

FIG. 1: The local crystal field strength at the planar oxygen site of the outermost CuO_2 plane of the Hg-family of cuprates. All results have been normalized by the maximum field which occurs for the $n = 3$ layer system.

To quantify the effect of the crystal environment in the parent systems, in Fig. 1. the local crystal field at the outermost CuO_2 layer for the $HgBa_2Ca_nCu_nO_{2(n+1)+\delta}$ (n = 1-6) family of cuprates is presented. Using experimental structural data[54] and assuming an ionic point charge model with formal valences assigned to each atom, the Ewald summation method[55] is used to perform the electrostatic sums for the Madelung energy and its variation along the c-axis, determining the electric field strength. As mentioned, the local field is zero in the single-layer compound, and rises for $n > 1$. A maximum is reached for $n = 3$ and decreasing field values are found for $n > 3$. (We note here that the reports for the structural data for the $n = 4$ and $n = 5$ compounds have a large degree of scatter, presumably from the difficulty in sample growth.)

This effect can be understood in terms of the spatial variation of the Madelung potential. The gradient of the Madelung potential, which determines the E-field in an electrostatic model, is identically zero at the mirror planes, which generically lie at the middle and edges of the unit cell. The electrostatic periodicity requires that a point of steepest decent of the Madelung energy exists at a location between these mirror planes.[57] Empirically, our Madelung potential calculations indicate that for $n = 1-3$ the outermost plane approaches this point of steepest decent and experiences a larger field due to the increased gradient. For $n > 3$ the outermost layer has passed this point and therefore experiences a reduced field for increasing n. Finally, as the number of layers continues to increase there is an overall reduction in the range of the amplitude of the Madelung potential variation such that a uniform profile in the limit of the infinite layer compound (such as $CaCuO_2$).

While it is noteworthy that this dependence of the local c-axis E-field mimics the variation of T_c in these compounds and that these c-axis phonons are the dominant phonons which provide pairing in the $d_{x^2-y^2}$ channel, the strength of the coupling determined from LDA, even with a factor of five enhancement, in no way can account for T_c itself. However it is an intriguing possibility that this electron-phonon coupling may provide a bootstrap to an underlying pairing mechanism dependent only upon the properties of the CuO_2 plane itself, and may directly impart a material dependence to T_c. Multiple pairing channels may then be required to explain superconductivity in the cuprates.[56] However, the relation between those channels, the role of correlations, and a formalism valid to describe superconductivity in the cuprates are all open problems central to the field for which definitive answers and methods are missing.

III. LAYER DEPENDENCE

In the previous section we discussed how the material dependence of the renormalizations is expected to arise in the various families of cuprates and how this coupling is expected to differ in the phonon and spin resonance proposals. We now wish to review the available ARPES data in light of the theoretical considerations of the previous section. Here, our focus is on the observed changes in the renormalizations as the number of layers within the Bi- and Tl-families.

Single crystals of nearly optimally doped $Tl_2Ba_2CaCu_2O_8$ (Tl-2212), $TlBa_2Ca_2Cu_3O_9$ (Tl-1223) and slightly overdoped $Tl_2Ba_2CuO_6$ (Tl-2201) were grown using the flux method. As-grown Tl2212 (T_c = 107 K) and Tl-1223 (T_c 123 K) crystals were chosen for the ARPES measurements. Tl-2201 crystals used in our measurement were prepared by annealing the as-grown crystal ($T_c \sim 30$ K) under a nitrogen flow at a temperature of 500°C, yielding a T_c of 80 K. The data were collected using a Scienta R4000 photoelectron spectrometer. Measurements were performed at the Stanford Synchrotron Radiation Lightsource (SSRL) beam line 5-4 using 28 eV photons and at the Advanced Light Source beam line 10.0.1 using 50 eV photons. The energy resolution was set at 15-20 meV for the Tl data presented in this work. Samples were cleaved and measured in ultrahigh vacuum ($< 4 \times 10^{-11}$ Torr.) to maintain a clean surface. Detailed ARPES results on these compounds have been reported in Ref. 46.

Although the dispersion kink along the nodal direction has been found universally in high-T_c cuprates,[3] the momentum dependence of this renormalization feature, when moving away from the nodal direction, exhibits a material dependence.[46,58] It has been confirmed recently that there is a dependence on the number of CuO_2 planes in the unit cell in the Bi-family and, most recently, in the Tl-family of cuprates.[46] In the multi-layer compounds, the kink becomes more dramatic and eventually breaks the band dispersion into two branches: one branch with a sharp peak and another branch with a broader hump structure .[4,7,10,46,58] The two branches asymptotically ap-

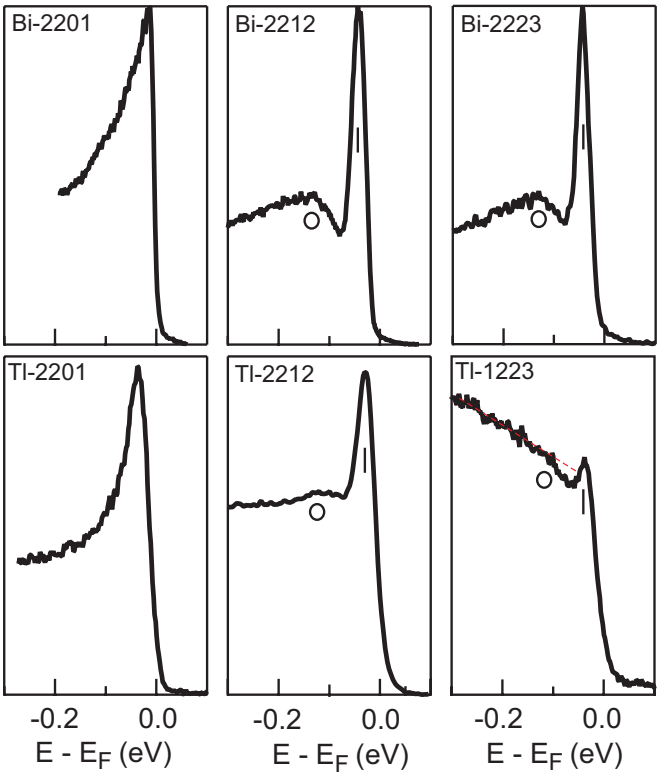

FIG. 2: Representative EDCs near the antinodal region of the Bi- and Tl-families of cuprates, including single layer (Bi-2201 and Tl-2201), bi-layer (Bi-2212 and Tl-2212), and tri-layer (Bi-2223 and Tl-1223) compounds. The high background in the data of Tl-1223 is probably due to the absence of a natural cleaving plane in the crystal structure. Nevertheless, a peak-dip-hump structure in the spectrum can still be discerned. The red dashed line is a guide-to-the-eye to make the "hump" more discernible.

proach one another at a characteristic energy scale of 70 meV and coincide with the dominant energy scale of the kink along the nodal dispersion for nearly optimally-doped cuprates. This separation of the band dispersion becomes most prominent near the antinodal region and results in the famous peak-dip-hump structure[11] in the energy distribution curves (EDCs), as shown in Fig. 2.

The momentum dependence of the kink is quite different in the single layer compound, where the dispersion kink becomes less prominent moving away from the node. In addition, the band dispersion retains a single branch with no separation observed, unlike the case of the multi-layer compounds.[59–61] As a result, no apparent peak-dip-hump structure can be seen in the EDCs near the antinodal region for the single layer compounds Fig. 2[60]. Similar results have been reported for optimal and underdoped LSCO[62–64] as well as overdoped Tl-2201.[65]

In summary, the layer dependent renormalization near the antinodal region is due most likely to electrons coupled to a sharp bosonic mode, whose origin is strictly constrained by the number of layers in the material. This mode is either absent, or has a negligible coupling to the electrons, in single layer compounds, but exhibits prominent coupling in the multi-layer compounds. The spin resonance mode does exist in some single layer cuprates[66] (notably Tl-2201 by not $La_2CuO_{4+\delta}$). Therefore, one can conclude that the spin resonance mode is an unlikely candidate for the mode responsible for the renormalizations in the antinodal region. On the other hand, coupling to c-axis phonons can exhibit a very different coupling in single- and multi-layer compounds. As we have discussed, the B_{1g} phonon couples strongly to the electrons in multi-layer compounds and weakly to electrons in single layer compounds. This mode can also reproduce the observed anisotropic momentum dependence of the renormalization in bi-layer Bi-2212.[25] We also note that the form for the B_{1g} coupling is attractive in the d-wave pairing channel,[48] which could be one factor enhancing T_c in the multi-layer systems.

IV. ENERGY SCALES AND DOPING DEPENDENCE

In the el-ph coupling picture the carriers couple to a spectrum of bosonic modes and we have already seen how the c-axis modes can produce a materials dependence of the renormalizations. It is important to note that the coupling to the out-of-plane bond buckling (B_{1g}) mode is highly anisotropic and may dominate the anti-nodal region in the normal state, and through the pile-up of the density of states at the gap edge, strengthens around the antinode and becomes visible in the nodal region, obscuring the in-plane bond-stretching (breathing) modes. Since these modes have different frequencies one would naturally expect the multiple energy scales to manifest in the experimental data. Indeed, evidence for multiple energy scales has been found both in the temperature dependence[7,25,26] as well as the doping dependence of Bi-2212.[8,15,29] In this section we revisit the doping dependence of the nodal and antinodal renormalizations, highlighting the different behavior in each region of the Brillouin zone and discuss how this dichotomy further supports the el-ph scenario.

High quality single crystals of optimally doped $Bi_2Sr_2Ca_{0.92}Y_{0.08}Cu_2O_{8+\delta}$ (Bi-2212 OP, T_c = 96 K) were grown by the floating zone method. The overdoped crystals with T_c = 88 K were prepared by post annealing the optimally doped Bi-2212 crystal under oxygen flow at a temperature of 400°C. The overdoped sample with T_c = 65K is a derivative of the Bi-2212 family with lead doped into the crystal to achieve such an overdoped configuration. The data were collected by using He I light (21.2 eV) from a monochromated and modified Gamma-data HE Lamp with a Scienta-2002 analyzer and in SSRL beamline 5-4 using 19 eV photons with a Scienta-200 analyzer. The energy resolution is ∼10 meV and angular resolution ∼0.35°. The samples were cleaved and mea-

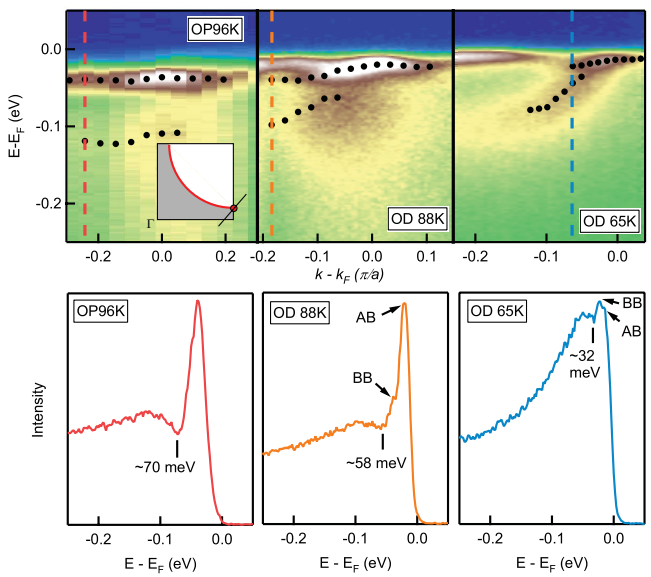

FIG. 3: The doping dependence of the antinodal spectrum of Bi-2212 taken in the superconducting state (10K). Shown in the upper row are the false color plots of the spectra taken along the indicated cut direction (inset). The black dots are the peak and hump positions of the bonding band seen in the EDCs. Shown in the lower row are the EDCs along the dashed line indicated in the false color plots. The symbols "AB" and "BB" represent the antibonding and binding bands while the numbers are the energy position of the dip of the EDC.

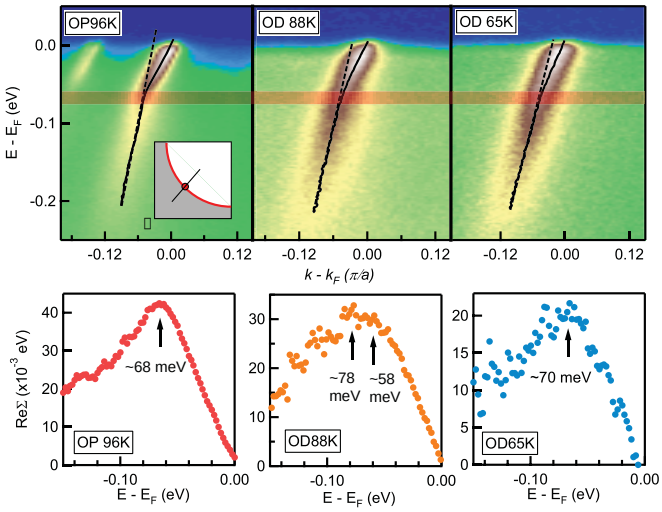

FIG. 4: The doping dependence of the nodal spectrum at a temperature well below T_c (10 K). Shown in the upper row are the false color plots of the spectra taken along the cut as indicated in the inset. The black curves are band dispersion obtained by fitting momentum dispersion curves (MDCs) to Lorentizan functions. The apparent kink position in the dispersion are marked by the yellow shaded area, which appears to be approximately the same for all three dopings. The dashed lines serve as a guide-to-the-eye for visualizing the apparent kink in the dispersion. Shown in the lower row are the real part of the self-energy extracted from subtracting the band dispersion from a linear bare band. The arrows indicate the positions of fine structure in the extracted ReΣ.

sured in ultra high vacuum ($< 4 \times 10^{-11}$ Torr.) to maintain a clean surface.

In Fig. 3 ARPES data taken along a cut in the antinodal region illustrate this effect. The upper panels show the measured spectral function along the cut while the lower panels show the ARPES spectral function $A(\mathbf{k}, \omega)$ at a fixed k-point as indicated by the dashed lines.

Near (0,π), the energy of the dip feature is the best measure of the energy scale of the mode responsible for the renormalization.[25,27] For the optimally doped sample (OP96K), shown in the first column of Fig. 3, the dip position is clearly located at $\omega \sim 70$ meV. This can be seen in both the false color plot and the EDC cut. For moderate overdoping (OD88K), the energy of the dip is lowered to $\sim$ 58 meV while for heavily overdoped (OD65K) the energy is lowered further to $\sim$ 32 meV. In both overdoped cases, contributions from the bonding- (BB) and anti-bonding (AB) bands contribute to the quasiparticle peak at the Fermi level. In the OD65K case, the contribution from the AB makes an exact determination of the dip position difficult and the estimate of $\sim$ 32 meV should be considered a lower bound.

Turning now to the nodal region, we find qualitatively different behavior. Fig. 4 presents $A(\mathbf{k}, \omega)$ along the nodal cut ((0,0) - (π,π)) for the same three samples. The highlighted region indicates the approximate position of the kink. In the nodal region the overall bandwidth is much larger than the energy of the bosonic modes so the dramatic band breakup does not occur[25] and the renormalization manifests as a kink in the dispersion. In this case, the energy scale of the kink is most easily determined from the structure of the real part of the self-energy ReΣ. The MDC-derived estimate for ReΣ, obtained from subtracting the MDC-derived dispersion from an assumed linear band, is also in the lower panels of Fig. 4.

The nominal doping dependence[67] of the energy scales in the nodal and antinodal region of Bi-2212 are summarized in Fig. 5a. For reference, the superconducting gap Δ_0 is shown also, which is determined from the peak positions of the Fermi function divided spectrum at the Fermi level. While the characteristic energy in the antinodal region (dip energy) follows the decrease in the superconducting gap, the characteristic energy in the nodal region remains more or less constant ($\sim$ 70 meV). The difference in the doping dependence of the two energy scales lends further support to the existence of coupling to multiple modes. If a single mode were responsible for the renormalization throughout the zone one would expect the doping dependence to follow the same trend in the nodal and antinodal regions.

The energy of the dominant mode Ω can be obtained by subtracting the magnitude of the superconducting gap from the observed energy scale, expected to be $\Omega + \Delta_0$.[25] The results of this procedure are shown in Fig. 5b. The

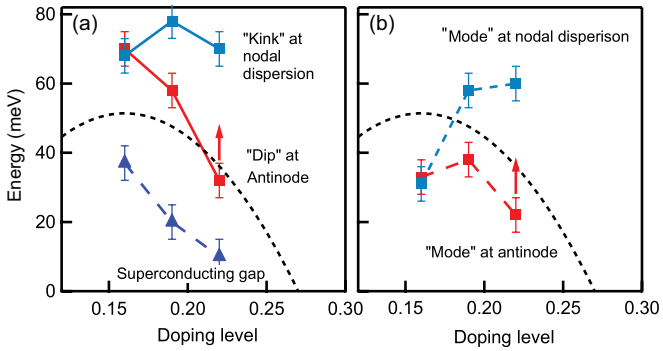

FIG. 5: A summary of some energy scales relevant to the renormalized band dispersions. (a) The apparent kink position in the nodal dispersion, dip energy at the antinodal region and the superconducting gap are summarized for the three doping levels shown in Fig 3. (b) the mode energy obtained by subtracting the superconducting gap from the characteristic energies of the renormalization effect. The red arrow is to remind the reader that the shown quantity at the antinodal region of the OD65K sample is a lower bound for the actual value.

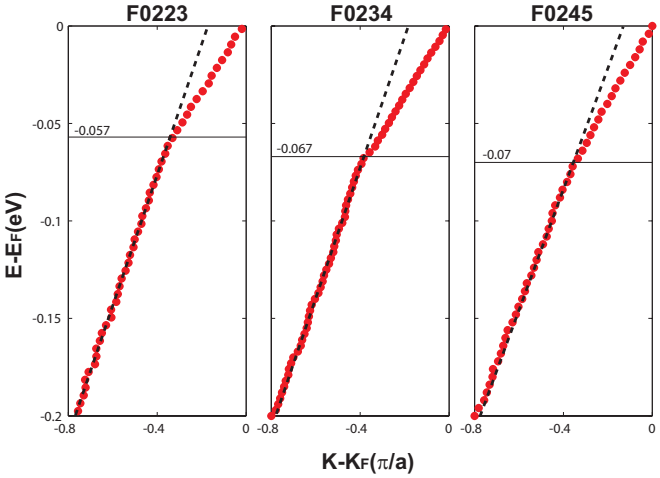

FIG. 6: MDC derived dispersions along the nodal direction (0,0) - (π,π) of the p-type band in the 3-layer (F0223), 4-layer (F0234) and 5-layer (F0245) F-family of cuprates.

energy of the dominant mode in the antinodal region, within the error bars of the data, is independent of doping. The behavior in the nodal region is different; the energy of the dominant mode changes with doping. At optimal doping the energy of the dominant mode is ~ 35 meV but in the overdoped samples the energy is larger ~ 60 meV. This result is consistent with the picture of coupling to multiple modes outlined in Ref. 25. We also note that in OD88K a secondary feature can be observed in ReΣ at precisely the same energy as the dip energy of the antinodal region. Similar fine structure was reported earlier in Ref. 26. The presence of this sub-feature in the UD88K data as the sample is progressively overdoped, along with the 35 meV scale in the nodal data at optimal doping, is evidence of a trade off between a coupling dominated by the B_{1g} mode and one dominated by the bond stretching mode. We further note that Ref. 8 reached similar conclusions but assigned the anti-nodal renormalizations to the spin resonance mode. We believe that the multi-layer data of the previous section, especially the single-layer Tl data which shows no renormalization in the anti-nodal region, directly refutes this conclusion and favors the el-ph scenario.

V. THE F-FAMILY OF MULTILAYER CUPRATES

In this final section we turn attention to aspects of the kink in the multi-layer F-family of cuprates with $n = 3-5$ CuO_2 layers. The single crystalline samples were grown by the flux method under high pressure.[68] ARPES measurements on the F-family were performed at beamline 10.0.1 of the Advance Light Source (ALS) at Lawrence Berkeley National Laboratory. The measurement pressure was kept $< 4 \times 10^{11}$ Torr at all time and data were recorded by Scienta R4000 Analyzers at 15K sample temperature. The total convolved energy and angle resolution were 16 meV and 0.2° respectively for photoelectrons generated by 55 eV photons.

In Fig. 6 MDC derived dispersions for p-type bands of the three ($Ba_2Ca_1Cu_2O_6(O,F)_2$, F0223), four ($Ba_2Ca_3Cu_4O_8(O,F)_2$, F0234) and five ($Ba_2Ca_4Cu_5O_{10}(O,F)_2$, F0245) layer F-based cuprates are presented. In all three cases the dispersions show clear kinks, but at increased energy scales in the four- and five-layer materials. As noted earlier, for a d-wave superconductor coupled to an Einstein mode, the energy scale of the kink occurs at $\Omega + \Delta_0$ where Ω is the energy of the mode and Δ_0 is the maximum value of the superconducting gap. Therefore the shift in energy is due to the change in the superconducting gap size as n varies from 3 to 5. In order to quantify the strength of the kink, slopes are extracted from the dispersion above and below the kink position, $d\epsilon/dk|_>$ and $d\epsilon/dk|_<$. An estimate for the relative coupling strength λ' is then given by:

$$\left.\frac{d\epsilon}{dk}\right|_{>} = (1+\lambda')\left.\frac{d\epsilon}{dk}\right|_{<}. \qquad (1)$$

This procedure produces $\lambda' = 0.89$, 0.75 and 0.49 for $n = 3$, 4 and 5 respectively. This trend is easily understood in the phonon scenario where the dominant mode in the superconducting state is the B_{1g} mode for which the coupling strength is proportional to the local crystal field. The observed decrease in coupling strength can be understood if one recalls the expected local field strength in the outer most layers (recall Fig. 1), which decreases for $n > 3$.

We now turn our attention to the identification of the carrier types in the inner and outer planes of F0234. Experimentally, the parent compound of F0234 is known to self-dope with the inner and outer planes having Fermi surfaces of different carrier type. A recent ARPES study[45] found that the p-type bands are bilayer split along the nodal direction. Since the inner planes are expected to have a stronger inter-planar coupling than the outer planes, the observation of bilayer splitting provides strong evidence that the inner layers are p-type while the outer layers are n-type. Furthermore, kinks in the nodal dispersion of both sets of planes were observed but the strength of the coupling in the n-type layer by a factor of two.

The doping of individual layers may be driven electrostatically from Madelung (site) energy differences between the inner and outer planes. In order to determine the Madelung potential Φ of each site we again employ the Ewald summation technique using the structural data from Ref. 68 and assigning formal valence charges to each atom. The Madelung potentials we obtain for a hole located on the inner planes are $\Phi^{ip}_{Cu} = -26.97$, $\Phi^{ip}_{O} = 19.61$ eV/$\mathring{A}$ while for a hole located on the outer planes we obtain $\Phi^{op}_{Cu} = -26.06$, $\Phi^{op}_{O} = 19.61$ eV/$\mathring{A}$. The corresponding values of the local crystal field at the inner and outer planar oxygen sites are $E^{ip}_z = 5.79 \times 10^{-2}$ and $E^{op}_z = 5.66 \times 10^{-1}$ eV/$\mathring{A}$. The difference in Madelung energies between the layers are $\Delta\Phi = \Phi^{op} - \Phi^{ip}$ are $\Delta\Phi_{Cu} = 0.91$, $\Delta\Phi_O = 1.09$ eV. A positive value for $\Delta\Phi$ indicate that holes will flow from the outer layer to the inner plane in order to minimize their electrostatic energy. Therefore, our results indicate that the outer layer is n-type while the inner layer p-type. Furthermore, the strength of the E-field in the outer layer is substantially larger than that of the inner layer and therefore the el-ph coupling of the n-type layer will be stronger, in agreement with experiment.

In order to determine the relative doping of the two sets of layers the Madelung energies are now used as input to a model tight-binding calculation. Our electrostatic calculations show that even though the separate Madelung energies of Cu and O are found to vary across the unit cell, these variations tend to cancel within each layer individually and there are no substantial differences in the charge transfer energy between Cu and O within each plane. Therefore, in the absence of coherent c-axis hopping, the bands may be treated in terms of the usual single-band downfolded tight-binding methods apart, from a layer-dependent shift of the site energies. The bands crossing the Fermi level are then determined by the four CuO_2 antibonding bands, with the outer planes shifted in energy and with all four coupled by an interplanar hopping term.

Rather than addressing the full multi-orbital problem, we take a 5-parameter tightbinding model for the low-energy dispersion[69] and uniformly shift the site energy of the bands associated with the outer planes by the amount indicated by our Ewald calculation. The usual inter-planar coupling term[70] is introduced at this level with $t_\perp(\mathbf{k}) = t_\perp(\cos(k_x a) - \cos(k_y a))^2/4$ and $t_\perp = 50$ meV. The resulting model Hamiltonian is

$$\begin{aligned} H &= \sum_{\alpha=1}^{4} \sum_{\mathbf{k},\sigma} (\epsilon_\alpha(\mathbf{k}) - \mu) d^\dagger_{\alpha,\sigma,\mathbf{k}} d_{\alpha,\sigma,\mathbf{k}} \\ &+ \sum_{<\alpha \neq \alpha'>} t_\perp(\mathbf{k}) d^\dagger_{\alpha,\sigma,\mathbf{k}} d_{\alpha',\sigma,\mathbf{k}} \end{aligned} \quad (2)$$

where $\alpha = 1 - 4$ is the plane index, $\epsilon_\alpha(\mathbf{k}) = \epsilon(\mathbf{k}) + \delta\epsilon$ for the outer planes and $\epsilon_\alpha(\mathbf{k}) = \epsilon(\mathbf{k})$ for the inner planes, $\delta\epsilon = \Delta\Phi/\epsilon(\infty)$ with $\epsilon(\infty) = 3.5$ the dielectric constant[52] and $< ... >$ is a sum over neighboring planes. Here, μ is the chemical potential which is adjusted to maintain the total filling of the parent compound. The resulting model is then diagonalized for $\delta\epsilon = 0.29$ in order to obtain the relative filling of the four planes. We obtain fillings of 0.68 and 1.32 for the inner and outer layers, respectively. Experimentally, the carrier concentration of the two sets of planes, determined from the Luttinger fraction, were reported in Ref.73 with dopings of 0.60 ± 0.04 and 0.4 ± 0.03, relative to half-filling, in the p- and n-type bands which is in agreement with our results.

To summarize, our straightforward electrostatic model predicts an inequivalent filling for the inner and outer layers of F0234 which is driven by differences in the crystal environment of the two types planes. Using structural data we find that the outer layers are expected to be of n-type while the inner layers are of p-type. The environmental asymmetry of the two sets of planes also results in differing electric field strengths with the n-type (outer) layer experiencing a larger el-ph coupling. Both of these trends are in line with the findings of Ref. 45. However, this calculation does predict a larger ratio of the coupling strengths in the two layers. This discrepancy is probably due to the fact that the redistribution of charge between the layers has not been feed back into the electrostatic calculation. Doing so will likely reduce the ratio of E-fields predicted by in the electrostatic calculation. However, such a feedback scheme will require further guidance as to the distribution of doped carriers in the plane and, at the moment, we are not aware of any reliable indication of such.

VI. CONCLUSIONS

In this work we have presented aspects of the material and doping dependence of the dispersion renormalizations in the nodal and antinodal regions of various single- and multi-layer cuprates. We have found that the strength of the nodal kink has a strong material dependence and varies with the number of layers present in the material. In general, the kink strength mirrors T_c, taking on a maximal value in the $n = 3$ compounds. The issue can be complicated further in the multi-layer cuprates,

where Madelung potential differences can lead to inequivalent dopings in the various layers. This can lead to further symmetry breaking across the CuO_2 planes, and results in different kink strength in the different layers within the same material. Using a simple tight-binding model and electrostatic calculations we have developed a picture of this phenomena in self-doped F0234, which is consistent with recent ARPES studies.

The renormalization in the antinodal region also shows a marked dependence on the number of layers present in the material and is unresolved in the single layer cuprates. This result is difficult to reconcile for coupling to the spin resonance mode, which is expected not to vary with the number of layers, but is naturally explained by coupling to the B_{1g} phonon when one considers the crystal structure of these materials.

Further evidence for multiple phonon modes was found in the doping dependence of Bi-2212. Here, the features in the nodal and antinodal regions exhibit different behavior. Once gap referenced, the energy scale in the nodal region changes from $\sim 35-40$ meV to $\sim 70-80$ meV as the sample is overdoped. This change of energy scales cannot be explained by coupling to a single mode and therefore rules out the spin resonance mode, at least as the sole player. In the phonon scenario this signifies a trade-off between dominant coupling to the B_{1g} mode near optimal doping and a dominant coupling to the bond stretching mode in the overdoped samples. The change of relative coupling is due to increased screening of the B_{1g} mode as the carrier concentration is increased.

Both the doping and materials dependence presented here provides compelling evidence that a spectrum of phonon modes are responsible for both the nodal and antionodal low-energy renormalizations observed in the cuprates.

VII. ACKNOWLEDGEMENTS

This work was supported by the US Department of Energy, Office of Basic Energy Science under contract DE-AC02-76SF00515. Portions of this research were carried out at the Stanford Synchrotron Radiation Lightsource (SSRL), a national user facility operated by Stanford University on behalf of the US Department of Energy, Office of Basic Energy Sciences. This research used resources of the National Energy Research Scientific Computing Center, which is supported by the Office of Science of the U.S. Department of Energy under Contract No. DE-AC02-05CH11231. S. J. and T.P.D. would like to acknowledge support from NSERC and SHARCNET.

[1] P. V. Bogdanov, A. Lanzara, S. A. Kellar, X. J. Zhou, E. D. Lu, W. J. Zheng, G. Gu, J.-I. Shimoyama, K. Kishio, H. Ikeda, R. Yoshizaki, Z. Hussain and Z.-X. Shen, Phys. Rev. Lett. **85**, 2581 (2000).

[2] P. D. Johnson, T. Valla, A. V. Fedorov, Z. Yusof, B. O. Wells, Q. Li, A. R. Moodenbaugh, G. D. Gu, N. Koshizuka, C. Kendziora, Sha Jian, D. G. Hinks, Phys. Rev. Lett. **87**, 177007 (2001).

[3] A. Lanzara, P. V. Bogdanov, X. J. Zhou, S. A. Kellar, D. L. Feng, E. D. Lu, T. Yoshida, H. Eisaki, A. Fujimori, K. Kishio, J.-I. Shimoyama, T. Noda, S. Uchida, Z. Hussain and Z.-X. Shen, Nature (London) **412**, 510 (2001).

[4] A. Kaminski, M. Randeria, J. C. Campuzano, M. R. Norman, H. Fretwell, J. Mesot, T. Sato, T. Takahashi and K. Kadowaki, Phys. Rev. Lett. **86**, 1070 (2001).

[5] T. Cuk, D. H. Lu, X. J. Zhou, Z.-X.Shen, T. P. Devereaux and N. Nagaosa, Phys. Stat. Sol. (b) **242** 11 (2005).

[6] D. S. Dessau, B. O. Wells, Z.-X. Shen, W. E. Spicer, A. J. Arko, R. S. List, D. B. Mitzi and A. Kapitulnik, Phys. Rev. Lett. **66**, 2160 (1991).

[7] T. Cuk, F. Baumberger, D. H. Lu, N. Ingle, X. J. Zhou, H. Eisaki, N. Kaneko, Z. Hussain, T. P. Devereaux, N. Nagaosa and Z.-X. Shen, Phys. Rev. Lett. **93**, 117003 (2004).

[8] A. D. Gromko, A. V. Fedorov, Y.-D. Chuang, J. D. Koralek, Y. Aiura, Y. Yamaguchi, K. Oka, Y, Ando and D. S. Dessau, Phys. Rev. B **68**, 174520 (2003).

[9] T. K. Kim, A. A. Kordyuk, S. V. Borisenko, A. Koitzsch, M. Knupfer, H. Berger and J. Fink, Phys. Rev. Lett. **91**, 167002 (2003).

[10] T. Sato, H. Matsui, T. Takahashi, H. Ding, H.-B. Yang, S.-C. Wang, T. Fujii, T. Watanabe, A. Matsuda, T. Terashima and K. Kadowaki, Phys. Rev. Lett. **91**, 157003 (2003).

[11] M. R. Norman, H. Ding, J. C. Campuzano, T. Takeuchi, M. Randeria, T. Yokoya, T. Takahashi, T. Mochiku and K. Kadowaki, Phys. Rev. Lett. **79**, 3506 (1997).

[12] S. V. Borisenko, A. A. Kordyuk, V. Zabolotnyy, J. Geck, D. Inosov, A. Koitzsch, J. Fink, M. Knupfer, B. Büchner, V. Hinkov, C. T. Lin, B. Keimer, T. Wolf, S. G. Chiuzbăain, L. Patthey and R. Follath, Phys. Rev. Lett. **96**, 117004 (2006);

[13] S. V. Borisenko, A. A. Kordyuk, A. Koitzsch, J. Fink, J. Geck, V. Zabolotnyy, M. Knupfer, B. Bücher, H. Berger, M. Falub, M. Shi, J. Krempasky and L. Patthey, Phys. Rev. Lett. **96**, 067001 (2006).

[14] A. A. Kordyuk, S. V. Borisenko, V. B. Zabolotnyy, J. Geck, M. Knupfer, J. Fink, B. Bücher, C. T. Lin, B. Keimer, H. Berger, A. V. Pan, S. Komiya and Y. Ando, Phys. Rev. Lett. **97**, 017002 (2006).

[15] W. Meevasana, N. J. C. Ingle, D. H. Lu, J. R. Shi, F. Baumberger, K. M. Shen, W. S. Lee, T. Cuk, H. Eisaki, T. P. Devereaux, N. Nagaosa, J. Zaanen and Z.-X. Shen, Phys. Rev. Lett. **96**, 157003 (2006).

[16] X. J. Zhou, J. Shi, T. Yoshida, T. Cuk, W. L. Yang, V. Brouet, J, Nakamura, N. Mannella, S. Komiya, Y. Ando, F. Zhou, W. X. Ti, J. W. Xiong, Z. X. Zhao, T. Sasagawa, T. Kakeshita, H. Eisaki, S. Uchida, A. Fujimori, Z. Zhang, E. W Plummer, R. B. Laughlin, Z. Hussain and Z.-X. Shen, Phys. Rev. Lett. **95**, 117001 (2005).

[17] T. Dahm, V. Hinkov, S. V. Borisenko, A. A. Kordyuk, V. B. Zabolotnyy, J. Fink, B. Büchner, D. J. Scalapino, W. Hanke and B. Keimer, Nature Physics **5**, 217 (2009).

[18] T. Valla, A. V. Fedorov, P. D. johnson, B. O. Wells, S. L. Hulbert, Q. Li, G. D. Gu and N. Koshizuka, Science **285**, 2110 (1999); We note that while a kink in the electronic band dispersion can be seen in the earlier data of Valla *et al.*, this paper focused on quantum critical behavior of the frequency-dependent imaginary part of the self-energy and does not make any mention of a kink. Further, the authors stressed a quantum critical self-energy form that does not contain any energy scale.

[19] P. W. Anderson, Science **316**, 1705 (2007).

[20] E. Schachinger, J. P. Carbotte and T. Timusk, Europhys. Lett. **86**, 67003 (2009).

[21] Ar. Abanov, A. V. Chubukov, M. Eschrig, M. R. Norman and J. Schmalian, Phys. Rev. Lett. **17**, 177002 (2002).

[22] H.-Y. Kee, S. A. Kivelson and G. Aeppli, Phys. Rev. Lett. **88**, 257002 (2002).

[23] K. Byczuk, M. Kollar, K. Held, Y.-F. Yang, I. A. Nekrasov, Th. Pruschke and D. Vollhardt, Nature Physics **3**, 168 (2007).

[24] H. Isasawa, J. F. Douglas, K. Sato, T. Masui, Y. Yoshida, Z. Sun, H. Eisaki, H Bando, A. Ino, M. Arita, K. Shimada, N. Namatame, M. Taniguchi, S. Tajima, S. Uchida, T. Saitoh, D. S. Dessau and Y Aiura, Phys. Rev. Lett. **101**, 157005 (2008).

[25] T. P. Devereaux, T. Cuk, Z.-X. Shen and N. Nagaosa, Phys. Rev. Lett. **93**, 117004 (2004).

[26] W. S. Lee, W. Meevasana, S. Johnston, D. H. Lu, I. M. Vishik, R. G. Moore, H. Hisaki, N. Kaneko, T. P. Devereaux and Z. X. Shen, Phys. Rev. B **77**, 140504(R) (2008).

[27] A. W. Sandvik, D. J. Scalapino and N. E. Bickers, Phys. Rev. B **69**, 94523 (2004).

[28] W. S. Lee, S. Johnston, T. P. Devereaux and Z.-X. Shen, Phys. Rev. B **75**, 195116 (2007).

[29] W. Meevasana, T. P. Devereaux, N. Nagaosa, Z.-X. Shen and J. Zaanen, Phys. Rev. B **74**, 174524 (2006).

[30] M. L. Kulić and O. V. Dolgov, Phys. Rev. B **71**, 092505 (2005).

[31] M. L. Kulić, Phys. Rep. **338**, 1 (2000); M. L. Kulić and R. Zeyher, Phys. Rev. B **49**, 4395 (1994); R. Zeyher and M. L. Kulić, Phys. Rev. B **53**, 2850 (1996);

[32] Z. B. Huang, W. Hanke, E. Arrigoni and D. J. Scalapino, Phys. Rev. B **68**, 220507(R) (2003).

[33] R. Heid, K.-P. Bohnen, R. Zeyher and D. Manske, Phys. Rev. Lett. **100**, 137001 (2008).

[34] R. Heid, R. Zeyher, D. Manske and K.-P. Bohnen, Phys. Rev. B **80** 024507 (2009).

[35] F. Giustino, M. L. Cohen and S. G. Louie, Nature **452**, 975 (2008).

[36] D. Reznik, G. Sangiovanni, O. Gunnarsson and T. P. Devereaux, Nature **455**, E6 (2008).

[37] R. S. Markiewicz, S. Sahrakorpi, M. Lindroos, H. Lin and A. Bansil, Phys. Rev. B **72**, 054519 (2005).

[38] J. Lee, K, Kujita, K. McElroy, J. A. Slezak, M. Wong, T. Aiura, H. Bando, M. Ishikado, T. Masui, J.-X. Zhu, A. V. Balatsky, H. Eisaki, S. Uchida and J. C. Davis, Nature (London) **442**, 546 (2006).

[39] N. Jenkins, Y. Fansano, C. Berthod, I. Maggio-Aprile, A. Piriou, E. Giannini, B. W. Hoogenboom, C. Hess, T. Cren and Ø. Fischer, arXiv:0909.0500v1 (2009).

[40] J.-X. Zhu, K. McElroy, J. Lee, T. P. Devereaux, Q. Si, J. C. Davis and A. V Balatsky, Phys. Rev. Lett. **97**, 177001 (2006).

[41] J.-X. Zhu, A. V. Balatsky, T. P. Devereaux, Q. Si, J. Lee, K. McElroy and J. C. Davis, Phys. Rev. B **73**, 014511 (2006).

[42] S. Pilgram, T. M. Rice and M. Sigrist, Phys. Rev. Lett. **97**, 117003 (2006).

[43] J. Hwang, T. Timusk and J. P. Carbotte, Nature **446**, E3 (2006).

[44] T. Hanaguri, K. Kohsaka, J. C. Davis, C. Lupien, I. Yamada, M. Azuma, M. Takano, K. Ohishi, M. Ono and H. Takagi, Nature Physics **3**, 865 (2007).

[45] Y. Chen, A. Iyo, W. Yang, A. Ino, S. Johnston, H. Eisaki, H. Namatame, M. Taniguchi, T. P. Devereaux, Z. Hussain and Z.-X. Shen, Phys. Rev. Lett. **103**, 036403 (2009).

[46] W. S. Lee, K. Tanaka, I. M. Vishik, D. H. Lu, R. G. Moore, H. Eisaki, A. Iyo, T. P. Devereaux and Z. X. Shen, Phys. Rev. Lett. **103**, 067003 (2009).

[47] L. Pintschovius, Phys. Stat. Sol. (b) **242**, 30 (2005) and references therein.

[48] T. P. Devereaux, A. Virosztek and A. Zawadowski, Phys. Rev. B **51**, 505 (1995); T. P. Devereaux, A. Virosztek and A. Zawadowski, Phys, Rev. B **59**, 14618 (1999).

[49] B. Friedl, C. Thomsen and M. Cardona, Phys. Rev. Lett. **65**, 915 (1990); E. Altendorf, X. K. Chen and J. C. Irwin, Phys. Rev. B **47**, 8140 (1993)

[50] H. A. Mook, M. Mostoller, J. A. Harvey, N. W. Hill, B. C. Chakoumakos, and B. C. Sales, Phys. Rev. Lett. **65**, 2712 (1990); N. Pyka, W. Reichardt, L. Pintschovius, G. Engel, J. Rossat-Mignod, and J. Y. Henry; Phys. Rev. Lett. **70**, 1457 (1993).

[51] T. P. Devereaux, A. Virosztek, A. Zawadowski, M. Opel, P. F. Müller, C. Hoffmann, R. Philipp, R. Nemetschek, R. Hackl, A. Erb, E. Walker, H. Berger and L. Forró, Solid State Comm. **108**, 407 (1998); M. Opel, R. Hackl, T. P. Devereaux, A. Virosztek, A. Zawadowski, A. Erb, E. Walker, H. Berger and L. Forró, Phys. Rev. B **60**, 9836 (1999).

[52] S. Johnston, F. Vernay and T. P. Devereaux, Euro. Phys. Lett. **86**, 37007 (2009); Y. Ohta, T. Tohyama and S. Maekawa, Phys. Rev. B **43**, 2968 (1991).

[53] O. K. Andersen, S. Y Savrasov, O. Jepsen and A. I. Liechtenstein, J. Low Temp. Phys. **105**, 285 (1996).

[54] Q. Huang, J. W. Lynn, Q. Xiong and C. W. Chu, Phys. Rev. B **52**, 462 (1995); P. G. Radaelli, J. L. Wagner, B. A. Hunter, M. A. Beno, G. S. Knapp, J. D. Jorgensen and D. G. Hinks, Physica C **216**, 29 (1993); A. R. Armstrong, W. I. F. David, I. Gameson, P. P. Edwards, J. J. Capponi, P. Bordet and M. Marezio, Phys. Rev. B **52**, 15551 (1995); M. Paranthaman and B. C. Chakoumakos, Jour. of Sol. State Chem. **122**, 221 (1996); Q. Huang, O. Chmaissem, J. J. Capponi, C. Chaillout, M. Marezio, J. L. Tholence and A. Santoro, Physica C **227**, 1 (1988).

[55] P. Ewald, Ann. Phys. **369**, 253 (1921).

[56] See, e.g., Y. Bang, Phys. Rev. B **78**, 075116 (2008).

[57] S. Johnston, F. Vernay, B. Moritz, T. P. Devereaux, Z.-X. Shen, N. Nagaosa and J. Zaanen, To Be Published.

[58] W. S. Lee *et al.*, in Band Renormalization Effect of Bi2223, edited by A. Bussmann-Holder and H. Keller, "High T_c Superconductors and Related Transition Metal Oxides". (Springer-verlag, Berlin Heidelberg, 2007).

[59] J. Wei, Y. Zhang, H. W. Ou, B. P. Xie, D. W. Shen, J. F. Zhao, L. X. Yang, M. Arita, K. Shimada, H. Namatame, M. Taniguchi, Y. Yoshida, H. Eisaki and D. L. Feng, Phys. Rev. Lett. **101**, 097005 (2008).

[60] The peak-dip-hump structure in the single-layer Bi-2201 is rather weak and appears abruptly in a narrow range of momentum space with a different energy scale than that along the nodal direction.[59] In addition, the issue of a peak- dip-

hump structure in the single-layer compound seems more uncertain, as the reported peak-dip-hump lineshape appears to be inconsistent among the literature.[59,71]

[61] J. Graf, M. d'Astuto, C. Jozwiak, D. R. Garcia, N. L. Saini, M. Krisch, K. Ikeuchi, A. Q. R. Baron, H. Eisaki and A. Lanzara, Phys. Rev. Lett. **100**, 227002 (2008).

[62] Y. X. Xiao, T. Sato, K. Terashima, H. Matsui, T. Takahaski, M. Kofu and K. Hirota, Physica C **463**, 44 (2007).

[63] M. Shi, J. Chang, S. Pailhés, M. R. Norman, J. C. Campuzano, M. Månsson, T. Claesson, O. Tjernberg, A. Bendounan, L. Patthey, N. Momono, M. Oda, M. Ido, C. Mudry and J. Mesot, Phys. Rev. Lett. **101**, 047002 (2008).

[64] T. Sato, K. Terashima, K. Nakayama, T. Takahashi, K. Kadowaki, M. Kofu and K. Hirota, Physica C **460**, 864 (2007).

[65] D. C. Peets, J. D. F. Mottershead, B. Wu, I. S. Elfimov, R. Liang, W. N. Hardy, D. A. Bonn, M. Raudsepp, N. J. C. Ingle and A. Damascelli, New Journ. Phys. **9**, 28 (2007).

[66] H. He, P. Bourges, Y. Sidis, C. Ulrich, L. P. Regnault, S Paihès, N. S. Berzigiarova, N. N. Kolesnikov and B. Keimer, Science **295**, 1045 (2002).

[67] The nominal doping level is estimated from T_c using the empirical law $T_c = T_c^{\max}[1 - 82.6(x - 0.16)^2]$.

[68] A. Iyo, M. Hirai, K. Tokiwa, T. Watanabe and Y. Tanaka, Supercond. Sci. Technol. **17**, 143 (2004).

[69] M. R. Norman, M. Randeria, H. Ding, J. C. Campuzano, Phys. Rev. B **52**, 615 (1995).

[70] T. Xiang and J. M. Wealthy, Phys. Rev. Lett. **77**, 4632 (1996).

[71] J. Meng, W. Zhang, G. Liu, L. Zhao, H. Liu, Z. Jia, W. Lu, Z. Dong, G. Wang, H. Zhang, Y. Zhou, Y. Zhu, X. Wang, Z. Zhao, Z. Xu, C. Chen and X. J. Zhou, Phys. Rev. B **79**, 024514 (2009).

[72] W. Xie, O. Jepsen, O. K. Andersen, Y. Chen and Z.-X. Shen, Phys. Rev. Lett. **98**, 047001 (2007).

[73] Y. Chen, A. Iyo, W. Yang, X. Zhou, D. Lu, H Eisaki, T. P. Devereaux, Z. Hussain and Z.-X. Shen, Phys. Rev. Lett. **97**, 236401 (2006).